Journal of Clinical and Translational Hepatology **2023** vol. 11(3) | 605–613
DOI: 10.14218/JCTH.2022.00346

Original Article

Augmenter of Liver Regeneration Monoclonal Antibody Promotes Apoptosis of Hepatocellular Carcinoma Cells

Li-Li Huang[1], Fei-Yang Luo[2], Wen-Qi Huang[3], Hui Guo[3], Qi Liu[3], Ling Zhang[1], Ai-Shun Jin[2] and Hang Sun[3*]

[1]Department of Nephrology, The Second Affiliated Hospital, Chongqing Medical University, Chongqing, China; [2]Department of Immunology, College of Basic Medicine, Chongqing Medical University, Chongqing, China; [3]Key Laboratory of Molecular Biology for Infectious Diseases, Ministry of Education, Institute for Viral Hepatitis, The Second Affiliated Hospital of Chongqing Medical University, Chongqing, China

Received: 22 July 2022 | **Revised:** 2 September 2022 | **Accepted:** 18 September 2022 | **Published online:** 4 January 2023

Abstract

Background and Aims: Hepatocellular carcinoma (HCC) is one of the most common types of cancer, often resulting in death. Augmenter of liver regeneration (ALR), a widely expressed multifunctional protein, has roles in liver disease. In our previous study, we reported that ALR knockdown inhibited cell proliferation and promoted cell death. However, there is no study on the roles of ALR in HCC. ***Methods:*** We used *in vitro* and *in vivo* models to investigate the effects of ALR in HCC as well as its mechanism of action. We produced and characterized a human ALR-specific monoclonal antibody (mAb) and investigated the effects of the mAb in HCC cells. ***Results:*** The purified ALR-specific mAb matched the predicted molecular weight of IgG heavy and light chains. Thereafter, we used the ALR-specific mAb as a therapeutic strategy to suppress tumor growth in nude mice. Additionally, we assessed the proliferation and viability of three HCC cell lines, Hep G2, Huh-7, and MHC97-H, treated with the ALR-specific mAb. Compared with controls, tumor growth was inhibited in mice treated with the ALR-specific mAb at 5 mg/kg, as shown by hematoxylin and eosin staining and terminal deoxynucleotidyl transferase dUTP nick end labeling. Simultaneous treatment with the ALR-specific mAb and adriamycin promoted apoptosis, whereas treatment with the ALR-specific mAb alone inhibited cell proliferation. ***Conclusions:*** The ALR-specific mAb might be a novel therapy for HCC by blocking extracellular ALR.

Citation of this article: Huang LL, Luo FY, Huang WQ, Guo H, Liu Q, Zhang L, *et al*. Augmenter of Liver Regeneration Monoclonal Antibody Promotes Apoptosis of Hepatocellular Carcinoma Cells. J Clin Transl Hepatol 2023;11(3)605–613. doi: 10.14218/JCTH.2022.00346.

Keywords: Hepatocellular carcinoma; Augmenter of liver regeneration; Monoclonal antibody; Apoptosis.

Abbreviations: ADC, antibody-drug conjugate; ADM, adriamycin; ALR, augmenter of liver regeneration; HCC, hepatocellular carcinoma; mAb, monoclonal antibody; RTCA, real time cell analysis; SPR, surface plasmon resonance.

[*]**Correspondence to:** Hang Sun, Key Laboratory of Molecular Biology for Infectious Diseases, Ministry of Education,Institute for Viral Hepatitis,The Second Affiliated Hospital of Chongqing Medical University, Chongqing 400010, China. ORCID: https://orcid.org/0000-0002-2302-1993. E-mail: 300613@cqmu.edu.cn

Introduction

Hepatocellular carcinoma (HCC) is one of the most common types of cancer,[1] and is estimated to be the fourth most frequent cause of cancer-related death worldwide.[2] Currently, many systemic therapies are available, including surgical resection, tumor ablation, and transcatheter arterial chemoembolization, with surgical resections remaining as the gold standard treatment.[3] However, surgery is an option only for patients with early-stage disease, and those with severe cirrhosis are not recommended for surgical resection. At the worst, recurrence and progression may occur, even after surgical resection.[3]

Tumor cells are different from normal cells in that they can proliferate indefinitely and take over organ functions. There is evidence suggesting that augmenter of liver regeneration (ALR),[4–7] a widely distributed pleiotropic protein that was originally identified as a hepatic growth factor, is involved in HCC. ALR is also known as growth factor ERV1-like.[8] Liver-specific deletion of ALR leads to steatohepatitis and HCC,[4] and ALR is highly expressed in the liver[9,10] where it has roles in cell survival, iron metabolism and other metabolic processes, and stem cell maintenance.[5,11] In our previous study, we reported that decreased ALR expression influenced the proliferation and the survival of human multiple myeloma cells.[12,13] However, it is unclear whether ALR has a role in HCC. We generated and characterized a human ALR monoclonal antibody (mAb) and investigated its effects on HCC cells. We then used an *in vivo* model to determine whether the ALR-specific mAb could induce apoptosis of HCC cells.

Methods

Construction of a human ALR-IgG-expressing vector and plasmid

Human ALR heavy and light chains were cloned into a pCDNA3.4 expression vector that contained the human cytomegalovirus intermediate-early promoter (Supplementary Fig. 1). The vector was suitable for stable and transient expression in mammalian hosts. The plasmid was purified using the TIANprep Mini Plasmid Kit II (Tiangen Biotech, Beijing, China). Plasmid DNA was sequenced and stored at −20°C

until use. The amino acid sequence of ALR heavy chain was EVQLQQSGASFTELVKPGASVKISCKASGYGYNMNWVKQSHGKGIWELSNINPYYGSTSYNQKFKGRATLTVELNSLTSEDSAVYYDKSSSTAYMCALENYSGSQSLYYSAMDYWGQGTSVTVSSAKTTPPSVYPLAPGCGDTTGSSVTLGCLVKGYFPESVTVTWNSGSLPSGVHTFPALLQSGLYTMSSSVTVPSSTWPSQTVTCSVAHPASSTTVDKKLEPRGPKIDPCPPCKECHKCPAPNLEGGPSVFIFPPNIKDVLMISLSPMVTCVVVDVSEDDPDVQISWFVNNVEVHTAQTQTHREDYNSTLRVVSALPIQHQDWMSGKEFKCKVNNKDLPAPIERTISKIKGLVRAPQVYILPPPAEQLSRKDVSLTCLAVGFSPEDISVEWTSNGHTEENYKNTAPVLDSDGSYFIYSKLDIKTSKWEKTDSFSCNVRHEGLHSFYLKKTISRSPGK. The amino acid sequence of ALR light chain was DIVSPSSLAVSVGEKVTMSCMSQKSSQSLLYSSNQKNYLAWYQSQGPKQPKLLIYWASTRESYYCGVPDRFTGSGSGTDFTLTISSVKAEDLAIQQYYRSPLTFGAGTKLELKRADAAPTVSIFPPSSEQLTSGGASVVCFLNNFYPKDLNVKWKIDGSERQNGVLNSWTDQDSKDSTYSMSSTLTLTKDEYERHNSYTCEATHKTSTSPIVKSFNRNEC.

Transfection of Expi293F cells and purification of human ALR IgG

For recombinant antibody production and purification, a pair of plasmids (pcDNA 3.4), including 15 μg heavy chain and 15 μg light chain plasmids separately expressing the ALR-specific mAb were transiently co-transfected into Expi293F cells (cat. no. A14528; ThermoFisher Scientific, Waltham, MA, USA) with ExpiFectamine 293 Reagent (cat. no. A14524; ThermoFisher Scientific). Cells were incubated at 37°C in a shaking incubator at 120 rpm with 5% CO_2. After 7 days, the supernatant containing the Ab was centrifuged at 1,000 ×*g* for 15 min at 4°C, followed by 5,000 ×*g* for 20 min at 4°C. The supernatant was passed through a 0.45 μm filtering unit and captured by protein G Sepharose with an ÄKTA purifier system (both GE Healthcare, Chicago, IL, USA). Bound Ab was eluted with citrate buffer, pH 2.7, dialyzed against phosphate-buffered saline (PBS) for 2 days, and stored at −80°C until use.

Expression and purification of recombinant human ALR (rhALR) protein

To optimize the expression conditions for GST-ALR (the fusion protein), *Escherichia. coli* cells carrying the human GST-ALR expression plasmid (pGEX-4 T-1, with N-terminal GST) were grown in fresh Luria-Bertani liquid medium containing 0.1 mg/mL ampicillin and 0.05 mg/mL chloramphenicol overnight at 37°C in a shaking incubator. The production of protein was induced with 1.0 mM isopropyl-β-D-thiogalactoside (Beyotime, Shanghai, China) for another 4 h, until the optical density at 600 nm was between 0.6 and 0.8. Bacteria were centrifuged and resuspended in 1× PBS. Bacterial cell walls were broken by ultrasonication. Supernatants and precipitates were collected and processed for 15% sodium dodecyl sulfate polyacrylamide gel electrophoresis (SDS-PAGE) (Supplementary Fig. 2A). Purified GST-ALR was obtained using a GST-tag Protein Purification Column (Beyotime), followed by washing with 20 mM reduced L-glutathione (Sigma-Aldrich, St. Louis, MO, USA) and purified with ÄKTA (GE Healthcare) overnight at 4°C to obtain the purified GST-ALR (Supplementary Fig. 2B). After dialysis against PBS for 2 days, GST-ALR was diluted to 1 mg/mL with PBS and processed for 15% SDS-PAGE (Supplementary Fig. 2C). The peptide sequence was NH_2-MRTQQKRDTKFREDCPPDREELGRHSWAVLHTLAAYYPDLPTPEQQQDAQFIHLFSKFYPCEECAEDLRKRLCRNHPDTRTRACFTQWLCHLHNEVNRKLGKPDFDCSKVDERWRDGWKDGSCDCOOH.

Silver staining and western blotting

To verify the purity of the ALR IgG, 20 μg ALR was processed for SDS-PAGE, and the bands were visualized by silver staining using the Fast Silver Stain Kit (Beyotime). For western blotting, proteins were extracted from cells using RIPA lysis buffer (Beyotime), and protein concentrations were determined with a bicinchoninic acid (BCA) Protein Assay (Beyotime). For western blotting, proteins (30 μg/well) were separated by SDS-PAGE, transferred to polyvinylidene fluoride membranes, blocked with 5% nonfat milk, and probed with ALR (1:1,000), Bax,1:2,000 (ab182733; Abcam, Cambridge, UK), Bcl-2, 1:2,000 (ab194583; Abcam), Cleaved caspase-3 (1:1,000; Cell Signaling Technology), and cleaved caspase-9 (1:1,000; Cell Signaling Technology) primary antibodies.

Antibody binding kinetics measured by surface plasmon resonance technology (SPR)

The binding kinetics and affinity of the ALR-specific mAb to the rhALR protein were analyzed by SPR (Biacore T200; GE Healthcare). We compared the antibody binding kinetics from the commercial recombinant protein (SRP6489; Sigma-Aldrich, UK) and our self-purified protein (ALR-GST) with the ALR-specific antibody. Purified rhALR was covalently immobilized to a CM5 sensor chip by amine coupling in 10 mM sodium acetate buffer, pH 4.0, for a final coupling level of 166 response units (RU). SPR assays were run at a flow rate of 30 L/m in HEPES buffer (cat. no. V900477-500 G; Sigma-Aldrich). Sensograms were fitted with Biacore X100 Evaluation Software (Version 2.0.2; GE Healthcare). For epitope mapping, the ALR-specific mAb was sequentially injected and monitored for binding activity to determine whether it recognized individual or closely situated epitopes. To examine competition with the ALR-specific mAb, rhALR was immobilized to a CM5 sensor chip and 166 RU. The mAb (1 μM) was injected onto the chip until steady-state binding was reached. The rhALR protein (5 μg/mL), which was produced and purified as described above, was injected for 60 sec.

Immunoelectron microscopy (IEM)

Huh 7 cells were fixed in IEM fixative (cat. no. G1124; Servicebio, Wuhan, China) at room temperature for 5 m. Cells were collected, transferred to a 1.5 mL Eppendorf tube, centrifuged at 1,000 rpm for 2 m, and fixed at room temperature for 30 m under dark conditions. Cells were centrifuged at 4°C and washed with prechilled 0.1 M PBS, pH 7.4, three times for 3 m each. A 2% low-melting-point agarose solution was prepared, cooled to about 40°C, and then added to cells. After dehydration with a graded series of ethanol solutions and infiltration with resin and xylol, samples were embedded in paraffin, and sectioned at 70–80 nm. Sections were incubated with the ALR-specific mAb (1:50) at 4°C overnight. On the following day, nickel grids were washed with TBS three times for 5 m each. Lastly, cells were incubated with 2% uranium acetate-saturated alcohol for 8 m under dark conditions, washed with 70% ethanol three times, and rinsed with ultrapure water three times. Nickel grids were observed by IEM, and images were acquired. Black particles (10 nm) were taken as positive signals.

Enzyme linked immunosorbent assay (ELISA)

For ELISA, 15-kDa rhALR (5 μg/mL; Sigma-Aldrich) was coated onto a 384-well plates that were stored overnight at 4°C. Thereafter, 100 μL of 5% bovine serum albumen (Beijing Solarbio Science and Technology Co., Ltd., Beijing, China) in PBST (PBS containing 0.05% Tween 20) was add-

ed to wells, and the plates were incubated at 37°C for 2 h. The ALR-specific mAb was diluted 1:10^2, 1:10^3, 1:10^4, 1:10^5, and 1:10^6 in PBST. After washing wells with PBST three times, 10 μl aliquots of each dilution were added to wells, and the plates were stored overnight 4°C. Wells were washed with PBST and incubated with a secondary anti-human IgG conjugated to horseradish peroxidase (Abcam) and PNPP buffer (ThermoFisher Scientific). The optical density (OD) at 405 nm was measured with a microplate reader (Molecular Devices, Sunnyvale, CA, USA). The ratio of the absorbance of the ALR-specific mAb to that of the control Ab greater than 2.1 was taken as specific binding of the Ab to the antigen.

Cell culture and treatment

Human Huh7 (RRID: CVCL-0336), MHCC97-H (RRID: CVCL-4972), and Hep G2 cells (RRID: CVCL-0027) were obtained from the Institute of Viral Hepatitis, Chongqing Medical University. The cell lines were authenticated using short tandem repeat following transfection (Genetica Cell Line Testing, USA), and tested negative for mycoplasma by MycoAlert@ Mycoplasma Detection Kit (Lonza, Madison, USA). The cells were cultured in Dulbecco's Modified Eagle's Medium (Gibco, Grand Island, NY, USA) supplemented with 10% fetal bovine serum (Moregate Biotech, Bulimba, QLD, Australia) and 1% penicillin/streptomycin (ThermoFisher Scientific) at 37°C in an incubator with 5% CO_2. Expi293F cells (ThermoFisher Scientific) were grown in Expi293 expression medium (ThermoFisher Scientific) at 37°C in a shaking incubator at 120 rpm with 5% CO_2. The ALR-specific mAb (0.1 μg/μL) and adriamycin (ADM; 0.004 mg/mL; MCE, Beijing, China) were added to the medium of the treatment group, and PBS was added to the control group. At the end of treatment, cells were harvested, and lysates were prepared for biochemical analysis.

Cell apoptosis assay

Cells treated with the ALR-specific mAb and/or doxorubicin were stained with the Annexin V-FITC/PI Staining Kit (BD Biosciences, Franklin Lakes, NJ, USA). Cells were resuspended in 1× binding buffer at a density of 1×10^6 cells/mL, incubated with 5 μL fluorescein isothiocyanate (FITC) and 10 μL propidium iodide at room temperature for 15 m, and then assayed by flow cytometry (FACS; Canto II; BD Biosciences).

Cell viability assay

The cell survival rate was determined with a Cell Counting Kit-8 (Dojindo Molecular Technologies, Rockville, MD, USA) according to the manufacturer's instructions. Cells (1×10^4) were plated in 96-well plates, incubated with different dilutions of the ALR-specific mAb (1:10, 1:50, 1:100, and 1:500; stock concentration, 1 μg/μL) at 37°C, and observed at 0, 24, 48, and 72 h. PBS served as the vehicle control. The OD at a wavelength of 450 nm was measured with a microplate reader. The percentage of living cells was calculated as a ratio of the absorbance of the treatment group to that of the control group.

Real time cell analysis (RTCA)

The cell survival rate was assayed with an RTCA kit (Agilent, Santa Clara, CA, USA). In brief, 50 μL of media was added to E-Plate 16 wells, and the background measurement was obtained. Cells (5×10^3) were plated and incubated with different dilutions of the ALR-specific mAb. The final volume in each well was 100 μL. Cells were observed for 3 days.

RNA isolation and real-time quantitative polymerase chain reaction (qPCR)

Total RNA of Huh 7 cells and total liver-tumor RNA from all groups were extracted with total RNA isolation kits (RNAeasy; Beyotime, China), and cDNA was synthetized using PrimeScript Reagent kits with gDNA Eraser (cat. no. RR047A; Takara Biotechnology Co., Ltd.) following standard protocols. Relative expression of target genes as determined by qPCR using SYBR Mixture (Takara Biotechnology Co., Ltd.) performed in 25 μL volumes with 2 μL cDNA, 400 nM of each sense and antisense primer and 12.5 μL Brilliant SYBR Green QPCR Master Mix (Takara Bio, Inc.) on an ABI PRISM 7000 sequence detection system (Applied Biosystems, ThermoFisher Scientific, Inc.). The reaction was performed for 40 cycles of denaturation at 95°C for 30 s, annealing at 53°C for 30 s and extension at 72°C for 10 s. Primer sequences are shown in Supplementary Table 1. All experiments were repeated at least in triplicate with three independent replicates for each group. To quantify gene expression, the $2^{-\Delta\Delta Ct}$ relative quantification method was used.

Transmission electron microscopy (TEM)

Huh-7 cells were plated in 10 cm dishes, treated as indicated, and fixed in 2.5% glutaraldehyde overnight at 4°C, followed by 1% cacodylate-buffered osmic acid in 0.1 M phosphate buffer, pH 7.4, for 3 h. Cells were dehydrated through a graded series of ethanol solutions for 20 m and embedded, and 60 nm continuous sections were stained with 2% uranyl acetate and lead citrate and examined by TEM (Hitachi, Tokyo, Japan).

Analysis of antitumor activity in vivo

Seven-week-old male BALB/c-nude mice (HFK Bioscience Co., Beijing, China) were used. All nude mice were maintained in a standard vivarium with cycles of 12 h light and 12 h dark, a temperature of 18–23°C, and a humidity of 40–60%. Mice had access to water and food *ad libitum*. Huh-7 cells (5×10^6) were injected subcutaneously into the right flank of nude mice and treatment was initiated when the tumor volume reached 100 mm^3. Five mice were used in each treatment group. ALR-specific mAb (2.5 mg/kg, 5 mg/kg) or PBS was administered directly into each tumor every 3 days. Body weight and tumor volume were measured. The size of the tumor mass was calculated in mm^3 as 0.5 × (length × $width^2$) using the two largest dimensions.

Histopathological analysis of tumors

Mice were sacrificed after treatment, tissues were fixed in 10% neutral buffered formalin, and sections were stained with hematoxylin and eosin.

Terminal deoxynucleotidyl transferase dUTP nick end labeling (TUNEL)

Tumors were harvested from mice and processed for TUNEL. Staining was performed on 2 μm formalin-fixed paraffin sections using the DeadEnd Fluorometric TUNEL System (Promega, Madison, WI, USA) according to the manufacturer's instructions. Images were acquired with a microscope (DS-U3; Nikon, Tokyo, Japan).

Statistical analysis

Statistical analysis was performed with Prism 8.0 software (GraphPad Software, La Jolla, CA, USA). Student's *t*-test was used for comparisons between two groups. Multivariate results were analyzed by one- or two-factor analysis of vari-

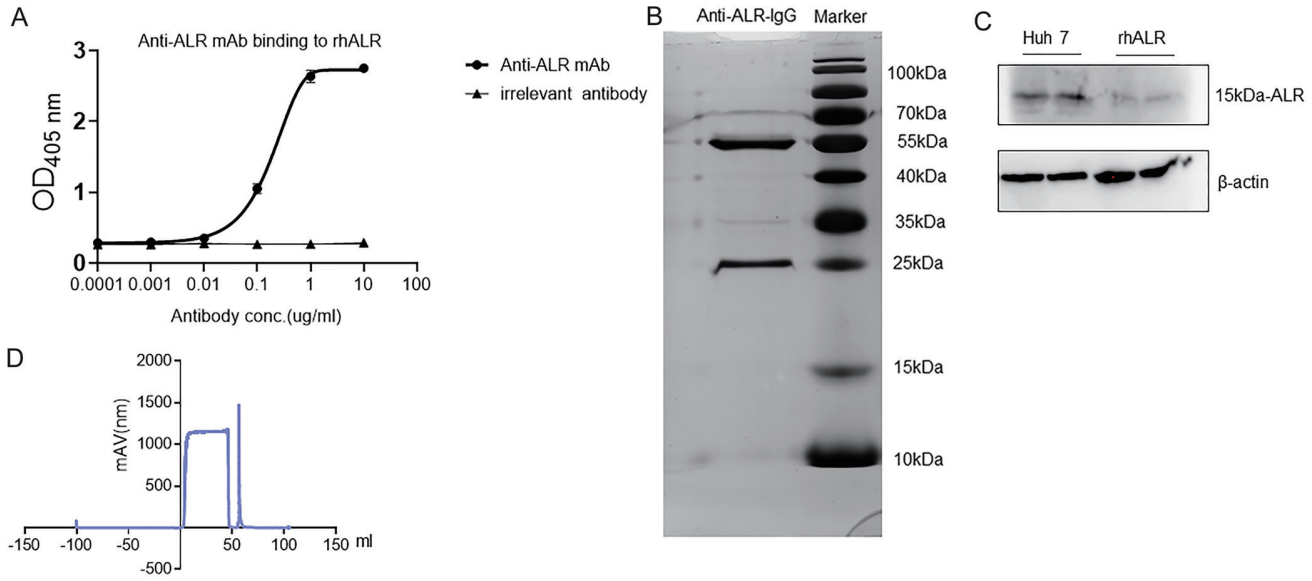

Fig. 1. Characterization of the ALR-specific mAb. (A) ELISA results show that the ALR-specific mAb bound specifically to the 15 kD rhALR protein. (B) Silver staining shows heavy and light chains of the IgG molecule. (C) Western blotting shows that the ALR-specific mAb bound specifically to the ALR protein in Huh 7 cells and commercial recombinant rhALR. (D) Purification of the ALR-specific mAb by ÄKTA.

ance, with Tukey's multiple comparison test. *P*-values <0.05 were considered statistically significant.

Results

Purification and verification of the ALR-specific mAb

Binding of the ALR-specific mAb to the rh-ALR protein as assessed by ELISA with a nonspecific human Ab (HBs Ag) as the control. When the OD at 405 nm <1, the results were taken as specific binding of the Ab to the antigen. As shown in Figure 1A, the titer of the ALR-specific mAb was 1 μg/mL. The OD of the control Ab was <1, indicating nonspecific binding between the Ab and the antigen. The silver staining results revealed one light chain (25 kDa) and one heavy chain (55 kDa) (Fig. 1B). The ALR-specific mAb (1:1,000) was used as the primary Ab for western blotting, which indicated that the antibody bound to the antigen. Commercial recombinant rhALR was the control (Fig. 1C). The ALR IgG was also successfully purified with an ÄKTA system (äkta FPLC, GE Healthcare) (Fig. 1D).

Immunoelectron microscopy and antibody binding kinetics

We examined the localization of ALR by IEM and found that the protein was mainly distributed in the cytoplasm and the nucleus of Huh 7 cells (Fig. 2A). We examined the antibody binding kinetics of ALR-specific mAb using GST-ALR protein that we produced, and a commercial rhALR recombinant protein. SPR using the ALR-specific mAb and GST-ALR showed that the ALR-specific mAb had a dissociation constant of approximately 10^{-8} (Fig. 2B). Two types of rhALR appear to correlate with dissociation constants. The antibody binding kinetics of the commercial recombinant protein had dissociation constants of about 10^{-7} (Supplementary Fig. 3)

Effects of the ALR-specific mAb on cell viability

Hep G2, Huh-7, and MHC97-H cells were treated with 1:10, 1:50, 1:100, and 1:500 dilutions of the ALR-specific mAb for 24, 48, and 72 h. At a dilution of 1:10, the survival rate was significantly lower than that of the other groups at all time points examined. Except at 1:500, the cell viability decreased significantly at all dilutions at 24 h. Cell viability was significantly increased at 48 h compared with 24 h (Fig. 3A). The ALR-specific mAb at a dilution of 1:10 and a treatment time of 24 h was used for subsequent experiments in Huh 7 cells (Fig. 3B), and the results were consistent with those shown in Figure 3A. RTCA was used to monitor changes in cell number and cell–substrate attachment strength, with the cell index (CI) reflecting the cell viability of different groups. To confirm the effects of the ALR-specific mAb on tumor cells, different cell lines were treated with different dilutions of the ALR-specific mAb. The CI of the 1:10 diluted group was lower than that of the other groups. Taken together, the results indicate that the ALR-specific mAb inhibited cell proliferation.

Effects of the ALR-specific mAb on cell apoptosis

A previous study reported that the recombinant ALR protein had anti-apoptotic activity.[14] Consequently, we assessed the effects of the ALR-specific mAb on cell death (Fig. 4A, B). There was no difference in the apoptotic rate, which included both early and late apoptotic cells, between groups after treatment with the ALR-specific mAb for 24 h. However, treatment with ADM (adriamycin) and the ALR-specific mAb promoted apoptosis. The expression of pro-apoptotic and anti-apoptotic proteins was examined by western blotting (Fig. 4C). Compared with controls, treatment with ADM increased Bax expression and decreased Bcl-2 expression. Additionally, the Bax level was significantly higher in the ADM-ALR-specific mAb group than that in the ADM group. TEM confirmed that apoptotic bodies were present after treatment with ADM and the ALR-specific mAb and were absent after treatment with the vehicle control (Fig. 4D). Apoptosis-associated protein was assayed in the four groups. Cells treated with 0.004 mg/mL ADM for 24 h triggered apoptosis compared with the PBS group. After blocking extracellular ALR by mAb, the expression of pro-apoptosis proteins was significantly increased (Fig. 4E), and similar results were seen with qPCR of Huh 7

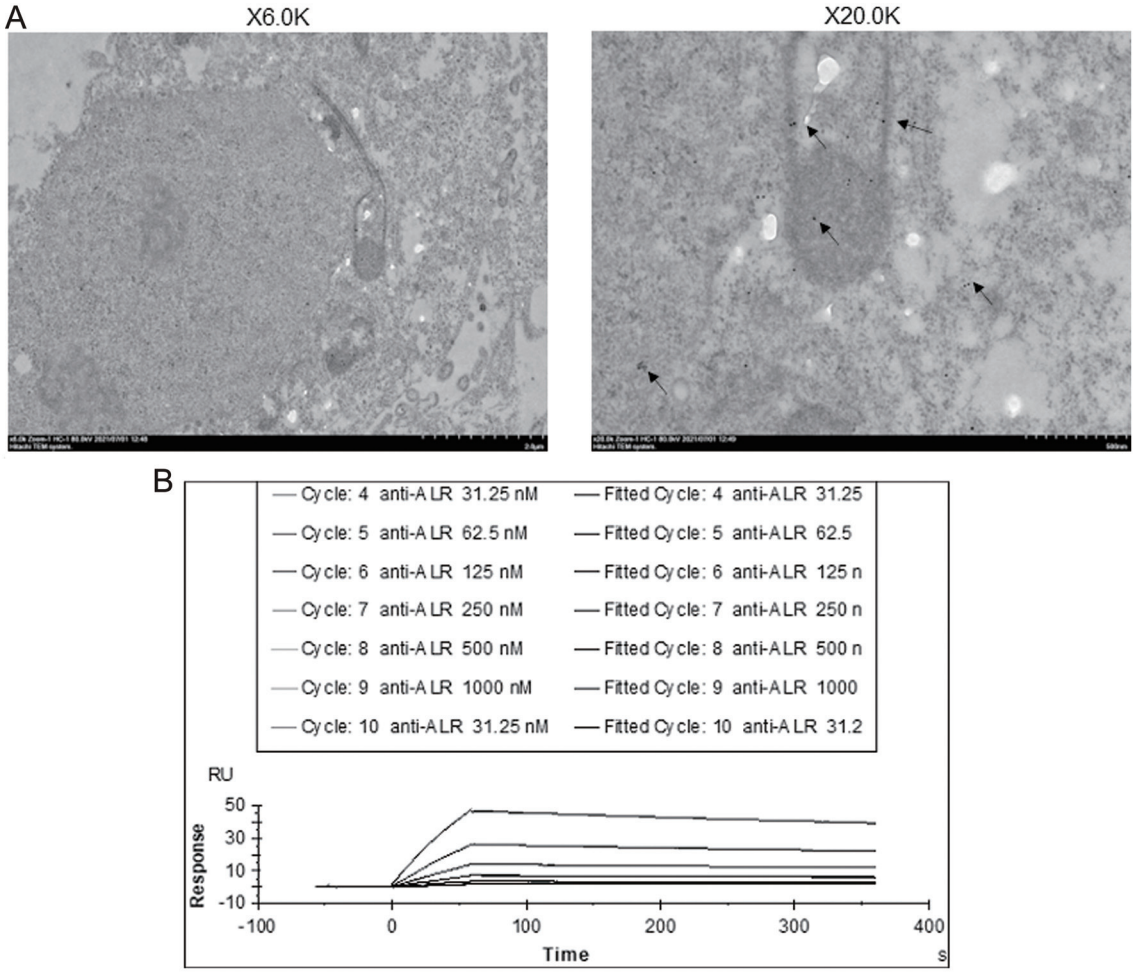

Fig. 2. Immune electron microscopy (IEM) and surface plasmon resonance (SPR) binding kinetics. (A) IEM results of Huh 7 cells. Black arrows indicate gold particles. Scale bars: 2 μm and 500 μm. (B) Binding kinetics of the ALR-specific mAb with the rhALR protein, as measured by SPR. The purified rhALR protein was immobilized onto a CM5 sensor chip, followed by the ALR-specific mAb. Black lines are experimentally derived curves; colored lines are fitted curves.

cells (Fig. 4F). Taken together, the results indicate that the ALR-specific mAb blocked secreted ALR, thereby increasing apoptosis after treatment with ADM.

Antitumor activity of the ALR-specific mAb

To assess the antitumor activity of the ALR-specific mAb *in vivo*, we assessed the potential of the mAb as a therapeutic entity in a tumor-bearing mouse model. BALB/cA-nude mice were inoculated subcutaneously with Huh 7 cells. Mice were treated with a single intravenous dose of the ALR-specific mAb when the tumor volume reached approximately 100 mm^3. Tumors grew more slowly in mice treated with the ALR-specific mAb at 5 mg/kg compared with mice treated with the ALR-specific mAb at 2.5 mg/kg, or PBS (Fig. 5A). Mice in the treatment groups did not have obviously abnormal body weights (Fig. 5B). Tumors were significantly smaller in mice treated with the ALR-specific mAb at 5 mg/kg than those in mice treated with PBS. The ALR-specific mAb significantly suppressed tumor growth compared with the control group (Fig. 5C, D). Tumor sections were processed for hematoxylin and eosin and TUNEL staining. Hematoxylin and eosin staining showed that tumor cells were widely distributed throughout the liver in PBS-treated mice. In contrast, nonviable tumor cells were observed centrally within tumors in ALR-specific mAb-treated mice. Furthermore, chromatin of necrotic cells formed dense hematoxylinophilic masses-pyknosis, and they may break up (Fig. 5E). Compared with the PBS-treated group, immunohistochemistry demonstrated that the expression of anti-apoptosis protein Bcl-2 was attenuated after administration of the ALR-specific mAb at 5 mg/kg (Fig. 5F). Additionally, apoptosis was examined by TUNEL. Compared with the PBS-treated group, extensive apoptosis was detected after administration of the ALR-specific mAb at 5 mg/kg (Fig. 5G). The expression of apoptosis-associated protein and genes were assayed by western blotting and qPCR. Compared with the PBS group, after administration of the ALR-specific mAb at 5 mg/kg expression of pro-apoptosis proteins increased significantly (Fig. 5H). The qPCR of tumors showed the same results (Fig. 5I).

Discussion

ALR is expressed by various tissues, including the liver, kidneys, and testes.[8,15] ALR is also present in the serum of mice with bacterial sepsis or hemorrhagic shock,[14] suggesting that it might serve as a diagnostic marker of hepatocellular stress and/or inflammation.[16–18] Equally important, the

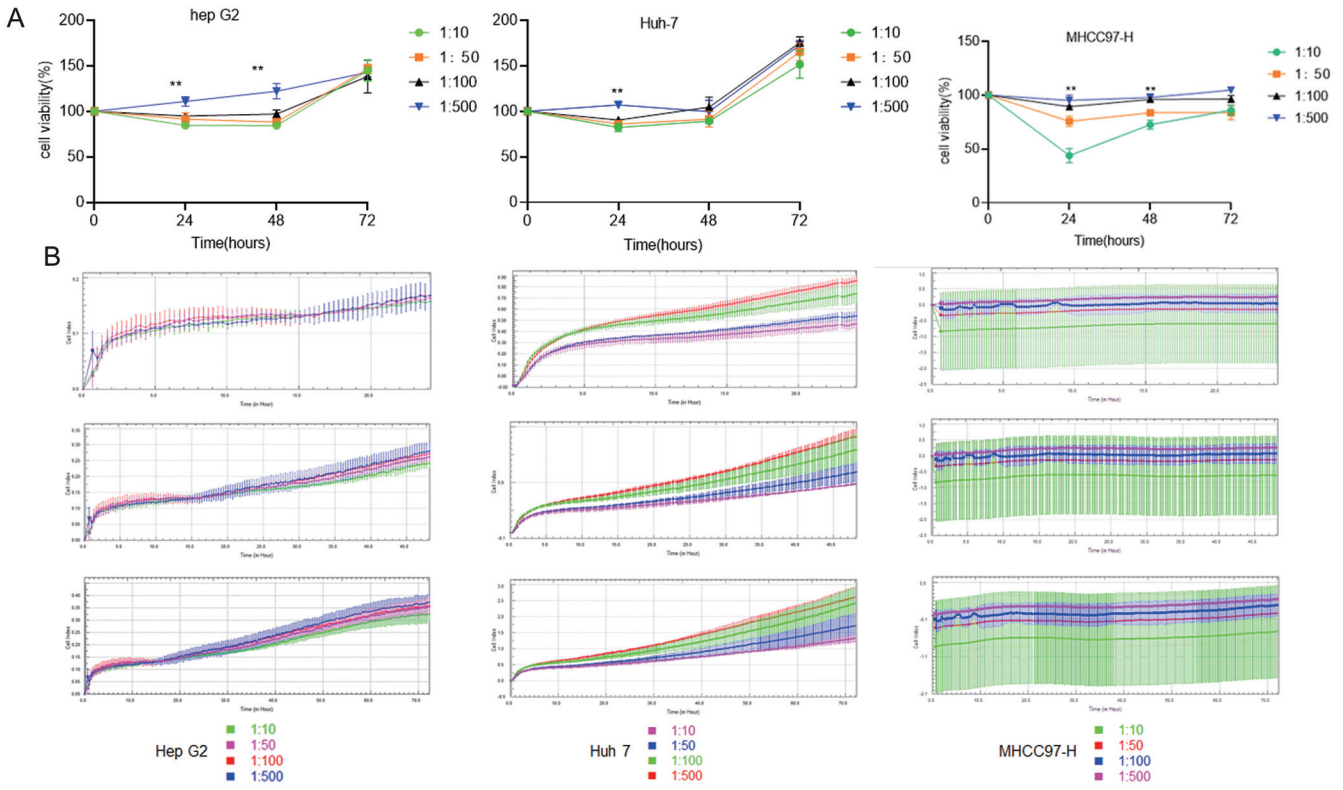

Fig. 3. Effects of the ALR-specific mAb on cell viability and proliferation. (A) HCC cells treated with the ALR-specific mAb at 1:10, 1:50, 1:100, and 1:500 dilution. $^{**}p<0.01$, 1:10 dilution vs. 1:500 dilution. (B) Real-time cell analysis of real-time changes.

expression of ALR is increased in a variety of tumors, including HCC,[19,20] leukemia,[21] colon cancer,[22] and pancreatic cancer.[23] A previous study reported that ALR had a protective effect on gliomas by exhibiting anti-apoptotic and anti-oxidative properties.[22] In a previous study, we demonstrated that ALR expression was higher in human multiple myeloma cells compared with human peripheral blood mononuclear cells.[13] Additionally, the ALR level was higher in myeloma cells than that in normal cells (unpublished data). Thus, ALR might be a potential biomarker in the treatment of specific diseases such as HCC.

ALR has 15 kD and 23 kD isoforms.[9,11,18,24,25] The long 23 kD form is predominantly found in the mitochondrial intermembrane space and is involved in a redox relay system, reduction of cytochrome c, and in regulation of the activities of certain proteins by its sulfhydryl oxidase activity as well as by inducing Fe/S maturation of proteins.[26] The short 15 kD form of human recombinant ALR is mainly found in the cytoplasm and nucleus.[27] Most important, it is secreted into extracellular environments, where it has important roles in liver regeneration, promotion of polyamine synthesis, and maintaining other physiological functions in cells.[26] It has been reported that ALR was as strong or stronger than transforming growth factor alpha (TGF-α) or human growth factor as a mitogen for hepatocytes.[27] In a previous study, we found that blocking extracellular 15-kD-ALR with an anti-ALR antibody decreased U266-cell proliferation in multiple myeloma by via the mitogen-activated protein kinase and cell cycle signaling pathways.[12] However, the role of ALR-specific mAb in HCC is not clear. In addition, although there are several treatments for HCC, including surgical resection, tumor ablation, transarterial therapy, and a variety of drugs, such as Sorafenib and Regorafenib, insufficient progress has been made in the treatment of HCC in part because it is difficult to maximize clinical benefits while minimizing adverse effects and cost.[3,28,29] In this study we first investigated the role of the ALR-specific mAb in HCC, using it to block the 15-kD isoform, which is a secreted protein, and found that the function of the 23-kD isoform was not affected. We purified and characterized the anti-ALR-specific mAb and investigated its effects on HCC. We found that the ALR-specific mAb inhibited the proliferation and promote the apoptosis of three HCC cell lines, consistent with a previous study in multiple myeloma cells[12] and another study that reported recombinant ALR had a protective role by up-regulating the expression of anti-apoptotic proteins during hepatogenesis in zebrafish.[30] ALR was found to significantly decrease cell death by inducing the expression of anti-apoptotic proteins, thereby inhibiting hepatocyte apoptosis.[31,32] ALR has also been shown to induce proliferation by enhancing polyamine synthesis.[33,34] In *in vitro* studies, compared with controls, the ALR-specific mAb suppressed cell growth and promote cell apoptosis, suggesting that the mechanism of action involved blocking extracellular ALR-increased tumor cell apoptosis. It is worth noting that, only in the case of ADM induced liver cancer cell damage, the ALR-specific mAb promoted the apoptosis of liver cancer cells by blocking extracellular ALR. This strategy selectively targets liver cancer cells under pathological rather than physiological conditions. The ALR-specific mAb does not affect normal liver cells and physiological processes. Future work taking advantage of this unique physiological feature may provide therapeutic potential. Additionally, antibody-drug conjugates (ADCs) are a class of drugs that combine a mAb with a cytotoxic drug, or payload, via chemical linkers.[35] Compared with

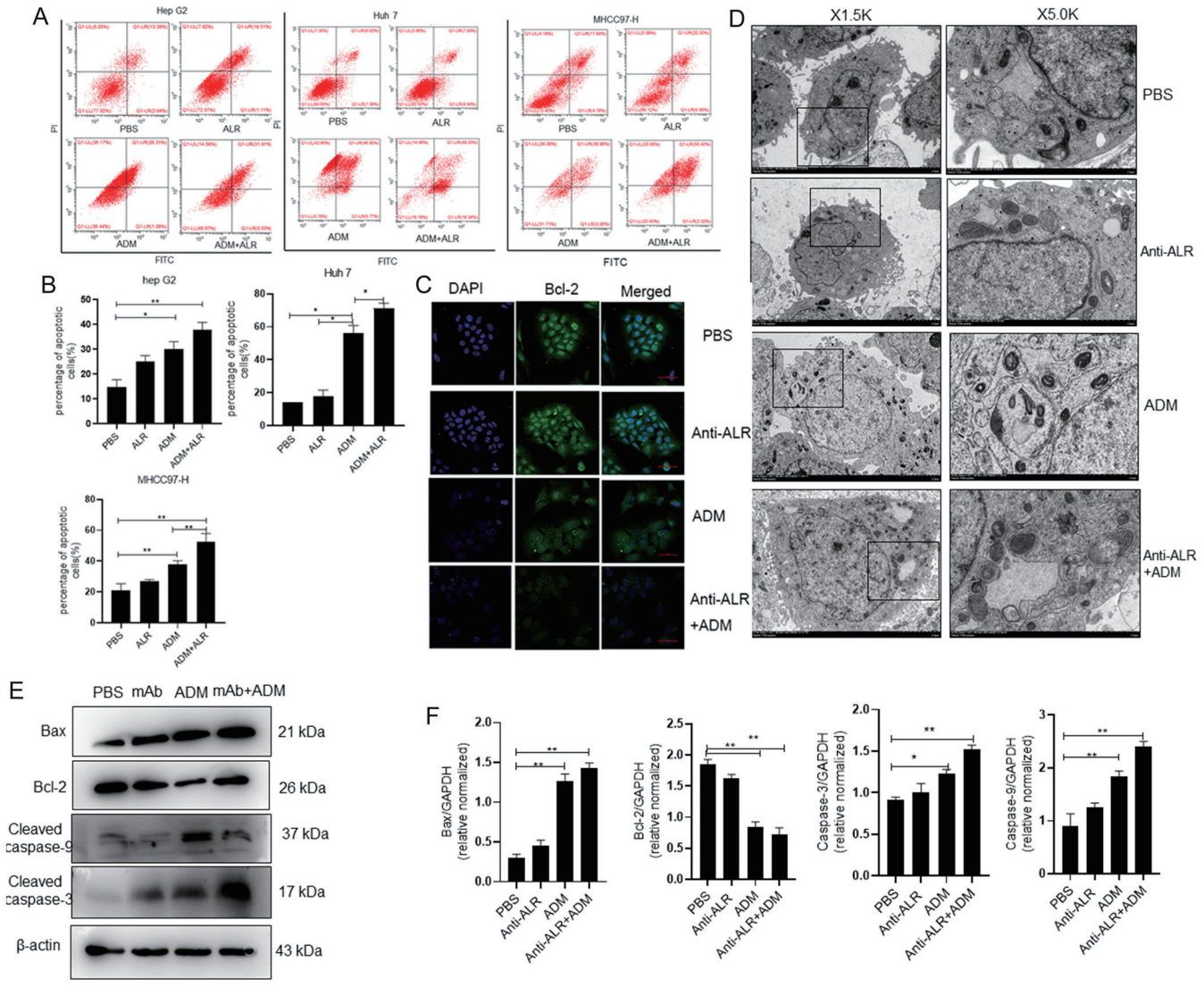

Fig. 4. Effects of the ALR-specific mAb on cell apoptosis. (A) HCC cells treated with the ALR-specific mAb at 1:10 (0.1 μg/μL) and/or ADM (0.004 mg/mL) for 24 h. $^{*}p<0.05$ and $^{**}p<0.01$. (B) Bar shows the apoptotic rate, including both early and late apoptotic cells, in different groups. (C) Bcl-2 expression and localization. Bcl2 expression was assayed by confocal laser-scanning microscopy. Scale bar, 50 μm. (D) Transmission electron microscopy of apoptotic bodies. Magnification, 1,500, 5,000. Scale bars, 5 μm or 2 μm. (E) Western blotting was used to estimate the expression of apoptosis-associated protein. (F) Real-time quantitative PCR was used to quantify expression levels of the apoptosis-associated gene in different groups.

traditional chemotherapeutic drugs, ADCs have higher anti-tumor activity and lower adverse effects.[36] Because of the specificity and the sensitivity of ADCs, such as ado-trastuzumab emtansine,[37,38] trastuzumab duocarmazine,[39,40] and MM-302,[41] they have a wider application in clinical settings. For instance, MM-302 is an Ab-liposomal drug that delivers PEGylated liposomal doxorubicin to tumors. Our study had several limitations. Although mice appeared healthy after the administration of the ALR-specific mAb, indicating no adverse effects on normal tissues, liver and kidney functions were not examined. Taken together, a better understanding of the mechanistic basis of the ALR-specific mAb may enable the design of rational combination therapies with other entities. In conclusion, ALR was involved in cell proliferation and cell survival in the context of HCC. The results provide evidence that blocking extracellular ALR inhibited cell proliferation and increased tumor cell apoptosis. The ALR-specific mAb might prove to be a novel therapy for HCC.

Funding

This work was supported by grants from the National Natural Science Foundation of China (81871608,30971334) and Postgraduate research and innovation projects of Chongqing Municipal Education Commission (CYB21178).

Conflict of interest

There are no conflicts of interest to declare.

Author contributions

Designed the study (HS, LZ, QL), performed the statistical analysis (LLH, WQH, HG), provided critical ideas for discus-

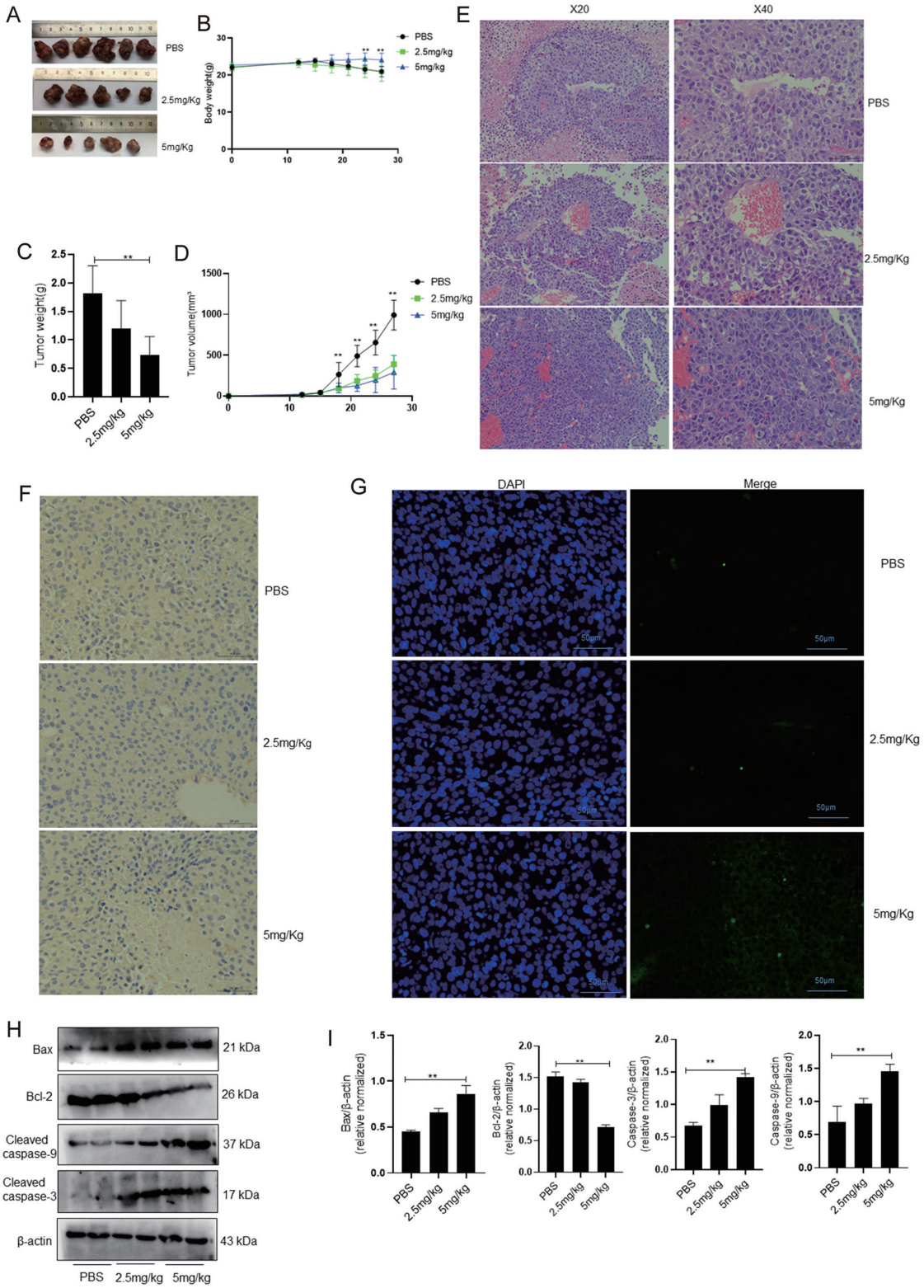

Fig. 5. Antitumor activity of the ALR-specific mAb in a xenograft tumor-bearing mouse model. (A) Antitumor efficacy of the ALR-specific mAb. At least five mice were included in each group. (B) Body weight of treated and control mice. (C) Tumor volume of treated and control mice. (D) Data points are means ± SEM of the tumor volume. $^{**}p<0.01$. (E) Histological analysis of tumor sections after treatment with the ALR-specific mAb or vehicle control. Scale bar, 50 μm (20×) or 100 μm (40×). (F) Immunohistochemistry of Bcl-2. Scale bar, 50 μm. (G) TUNEL showing apoptosis. Scale bar, 50 μm. (H) Western blotting was used to estimate the expression of apoptosis-associated protein from tumors. (I) Real-time quantitative PCR was used to quantify expression levels of the apoptosis-associated gene in tumors.

sion and technical support (FYL), drafted the manuscript and generated the figures (LLH, ASJ), critical revision of the manuscript for important intellectual content and agreed on the final version of the manuscript (all authors), corresponding author, approved the manuscript on behalf of all authors (HS).

Ethical statement

All experimental procedures were approved by the Institutional Review Committee of Chongqing Medical University (approval no. 2020,183) and adhered to the National Institutes of Health Guide for the Care and Use of Laboratory Animals.

Data sharing statement

We are happy to share reagents and sequence information presented in this study upon reasonable request.

References

[1] El-Serag HB, Rudolph KL. Hepatocellular carcinoma: epidemiology and molecular carcinogenesis. Gastroenterology 2007;132(7):2557–2576. doi:10.1053/j.gastro.2007.04.061, PMID:17570226.

[2] McGuire S. World Cancer Report 2014. Geneva, Switzerland: World Health Organization, International Agency for Research on Cancer, WHO Press, 2015. Adv Nutr 2016;7(2):418–419. doi:10.3945/an.116.012211, PMID:26980827.

[3] Villanueva A. Hepatocellular Carcinoma. N Engl J Med 2019;380(15):1450–1462. doi:10.1056/NEJMra1713263, PMID:30970190.

[4] Gandhi CR, Chaillet JR, Nalesnik MA, Kumar S, Dangi A, Demetris AJ, *et al*. Liver-specific deletion of augmenter of liver regeneration accelerates development of steatohepatitis and hepatocellular carcinoma in mice. Gastroenterology 2015;148(2):379–391.e374. doi:10.1053/j.gastro.2014.10.008, PMID:25448926.

[5] Nalesnik MA, Gandhi CR, Starzl TE. Augmenter of liver regeneration: A fundamental life protein. Hepatology 2017;66(1):266–270. doi:10.1002/hep.29047, PMID:28085209.

[6] Wu X, Liu G, Mu M, Peng Y, Li X, Deng L, *et al*. Augmenter of Liver Regeneration Gene Therapy Using a Novel Minicircle DNA Vector Alleviates Liver Fibrosis in Rats. Hum Gene Ther 2016;27(11):880–891. doi:10.1089/hum.2016.006, PMID:27136973.

[7] Zhang C, Huang J, An W. Hepatic stimulator substance resists hepatic ischemia/reperfusion injury by regulating Drp1 translocation and activation. Hepatology 2017;66(6):1989–2001. doi:10.1002/hep.29326, PMID:28646508.

[8] Gupta P, Venugopal SK. Augmenter of liver regeneration: A key protein in liver regeneration and pathophysiology. Hepatol Res 2018;48(8):587–596. doi:10.1111/hepr.13077, PMID:29633440.

[9] Thirunavukkarasu C, Wang LF, Harvey SA, Watkins SC, Chaillet JR, Prelich J, *et al*. Augmenter of liver regeneration: an important intracellular survival factor for hepatocytes. J Hepatol 2008;48(4):578–588. doi:10.1016/j.jhep.2007.12.010, PMID:18272248.

[10] LaBrecque DR, Steele G, Fogerty S, Wilson M, Barton J. Purification and physical-chemical characterization of hepatic stimulator substance. Hepatology 1987;7(1):100–106. doi:10.1002/hep.1840070121, PMID:3804188.

[11] Ibrahim S, Weiss TS. Augmenter of liver regeneration: Essential for growth and beyond. Cytokine Growth Factor Rev 2019;45:65–80. doi:10.1016/j.cytogfr.2018.12.003, PMID:30579845.

[12] Huang W, Sun H, Hu T, Zhu D, Long X, Guo H, *et al*. Blocking the short isoform of augmenter of liver regeneration inhibits proliferation of human multiple myeloma U266 cells via the MAPK/STAT3/cell cycle signaling pathway. Oncol Lett 2021;21(3):197. doi:10.3892/ol.2021.12458, PMID:33574936.

[13] Zeng HQ, Luo Y, Lou SF, Liu Q, Zhang L, Deng JC. Silencing of augmenter of liver regeneration inhibited cell proliferation and triggered apoptosis in U266 human multiple myeloma cells. Braz J Med Biol Res 2017;50(10):e6139. doi:10.1590/1414-431X20176139, PMID:28876364.

[14] Vodovotz Y, Prelich J, Lagoa C, Barclay D, Zamora R, Murase N, *et al*. Augmenter of liver regeneration (ALR) is a novel biomarker of hepatocellular stress/inflammation: in vitro, in vivo and in silico studies. Mol Med 2013;18(1):1421–1429. doi:10.2119/molmed.2012.00183, PMID:23073658.

[15] Hagiya M, Francavilla A, Polimeno L, Ihara I, Sakai H, Seki T, *et al*. Cloning and sequence analysis of the rat augmenter of liver regeneration (ALR) gene: expression of biologically active recombinant ALR and demonstration of tissue distribution. Proc Natl Acad Sci U S A 1994;91(17):8142–8146. doi:10.1073/pnas.91.17.8142, PMID:8058770.

[16] Fausto N, Campbell JS, Riehle KJ. Liver regeneration. Hepatology 2006;43(2 Suppl 1):S45–S53. doi:10.1002/hep.20969, PMID:16447274.

[17] Ring A, Stremmel W. The hepatic microvascular responses to sepsis. Semin Thromb Hemost 2000;26(5):589–94. doi:10.1055/s-2000-13215, PMID:11129415.

[18] Nguyen KH, Nguyen AH, Dabir DV. Clinical Implications of Augmenter of Liver Regeneration in Cancer: A Systematic Review. Anticancer Res 2017;37(7):3379–3383. doi:10.21873/anticanres.11704, PMID:28668825.

[19] Cao Y, Fu YL, Yu M, Yue PB, Ge CH, Xu WX, *et al*. Human augmenter of liver regeneration is important for hepatoma cell viability and resistance to radiation-induced oxidative stress. Free Radic Biol Med 2009;47(7):1057–1066. doi:10.1016/j.freeradbiomed.2009.07.017, PMID:19616613.

[20] Yu HY, Xiang DR, Huang HJ, Li J, Sheng JF. Expression level of augmenter of liver regeneration in patients with hepatic failure and hepatocellular carcinoma. Hepatobiliary Pancreat Dis Int 2010;9(5):492–498. PMID:20943458.

[21] Shen Y, Liu Q, Sun H, Li X, Wang N, Guo H. Protective effect of augmenter of liver regeneration on vincristine-induced cell death in Jurkat T leukemia cells. Int Immunopharmacol 2013;17(2):162–167. doi:10.1016/j.intimp.2013.05.030, PMID:23810409.

[22] Gatzidou E, Mantzourani M, Giaginis C, Giagini A, Patsouris E, Kouraklis G, *et al*. Augmenter of liver regeneration gene expression in human colon cancer cell lines and clinical tissue samples. J BUON 2015;20(1):84–91. PMID:25778301.

[23] Pan LF, Yu L, Wang LM, He JT, Sun JL, Wang XB, *et al*. Augmenter of liver regeneration (ALR) regulates acute pancreatitis via inhibiting HMGB1/TLR4/NF-κB signaling pathway. Am J Transl Res 2018;10(2):402–410. PMID:29511434.

[24] Mordas A, Tokatlidis K. The MIA pathway: a key regulator of mitochondrial oxidative protein folding and biogenesis. Acc Chem Res 2015;48(8):2191–2199. doi:10.1021/acs.accounts.5b00150, PMID:26214018.

[25] Gatzidou E, Kouraklis G, Theocharis S. Insights on augmenter of liver regeneration cloning and function. World J Gastroenterol 2006;12(31):4951–4958. doi:10.3748/wjg.v12.i31.4951, PMID:16937489.

[26] Gandhi CR. Augmenter of liver regeneration. Fibrogenesis Tissue Repair 2012;5(1):10. doi:10.1186/1755-1536-5-10, PMID:22776437.

[27] Verma AK, Sharma A, Subramaniyam N, Gandhi CR. Augmenter of liver regeneration: Mitochondrial function and steatohepatitis. J Hepatol 2022;77(5):1410–1421. doi:10.1016/j.jhep.2022.06.019, PMID:35777586.

[28] Yang JD, Hainaut P, Gores GJ, Amadou A, Plymoth A, Roberts LR. A global view of hepatocellular carcinoma: trends, risk, prevention and management. Nat Rev Gastroenterol Hepatol 2019;16(10):589–604. doi:10.1038/s41575-019-0186-y, PMID:31439937.

[29] Kulik L, El-Serag HB. Epidemiology and Management of Hepatocellular Carcinoma. Gastroenterology 2019;156(2):477–491.e471. doi:10.1053/j.gastro.2018.08.065, PMID:30367835.

[30] Li Y, Farooq M, Sheng D, Chandramouli C, Lan T, Mahajan NK, *et al*. Augmenter of liver regeneration (alr) promotes liver outgrowth during zebrafish hepatogenesis. PLoS One 2012;7(1):e30835. doi:10.1371/journal.pone.0030835, PMID:22292055.

[31] Ilowski M, Kleespies A, de Toni EN, Donabauer B, Jauch KW, Hengstler JG, *et al*. Augmenter of liver regeneration (ALR) protects human hepatocytes against apoptosis. Biochem Biophys Res Commun 2011;404(1):148–152. doi:10.1016/j.bbrc.2010.11.083, PMID:21108930.

[32] Polimeno L, Pesetti B, Annoscia E, Giorgio F, Francavilla R, Lisowsky T, *et al*. Alrp, a survival factor that controls the apoptotic process of regenerating liver after partial hepatectomy in rats. Free Radic Res 2011;45(5):534–549. doi:10.3109/10715762.2011.555482, PMID:21291353.

[33] Dayoub R, Thasler WE, Bosserhoff AK, Singer T, Jauch KW, Schlitt HJ, *et al*. Regulation of polyamine synthesis in human hepatocytes by hepatotrophic factor augmenter of liver regeneration. Biochem Biophys Res Commun 2006;345(1):181–187. doi:10.1016/j.bbrc.2006.04.040, PMID:16677602.

[34] Francavilla A, Vujanovic NL, Polimeno L, Azzarone A, Iacobellis A, Deleo A, *et al*. The in vivo effect of hepatotrophic factors augmenter of liver regeneration, hepatocyte growth factor, and insulin-like growth factor-II on liver natural killer cell functions. Hepatology 1997;25(2):411–415. doi:10.1002/hep.510250225, PMID:9021955.

[35] Chau CH, Steeg PS, Figg WD. Antibody-drug conjugates for cancer. Lancet 2019;394(10200):793–804. doi:10.1016/s0140-6736(19)31774-x, PMID:31478503.

[36] Thomas A, Teicher BA, Hassan R. Antibody-drug conjugates for cancer therapy. Lancet Oncol 2016;17(6):e254–e262. doi:10.1016/s1470-2045(16)30030-4, PMID:27299281.

[37] Verma S, Miles D, Gianni L, Krop IE, Welslau M, Baselga J, *et al*. Trastuzumab emtansine for HER2-positive advanced breast cancer. N Engl J Med 2012;367(19):1783–1791. doi:10.1056/NEJMoa1209124, PMID:23020162.

[38] Krop IE, Kim SB, Martin AG, LoRusso PM, Ferrero JM, Badovinac-Crnjevic T, *et al*. Trastuzumab emtansine versus treatment of physician's choice in patients with previously treated HER2-positive metastatic breast cancer (TH3RESA): final overall survival results from a randomised open-label phase 3 trial. Lancet Oncol 2017;18(6):743–754. doi:10.1016/s1470-2045(17)30313-3, PMID:28526538.

[39] Pondé N, Aftimos P, Piccart M. Antibody-Drug Conjugates in Breast Cancer: a Comprehensive Review. Curr Treat Options Oncol 2019;20(5):37. doi:10.1007/s11864-019-0633-6, PMID:30931493.

[40] Banerji U, van Herpen CML, Saura C, Thistlethwaite F, Lord S, Moreno V, *et al*. Trastuzumab duocarmazine in locally advanced and metastatic solid tumours and HER2-expressing breast cancer: a phase 1 dose-escalation and dose-expansion study. Lancet Oncol 2019;20(8):1124–1135. doi:10.1016/s1470-2045(19)30328-6, PMID:31257177.

[41] Geretti E, Leonard SC, Dumont N, Lee H, Zheng J, De Souza R, *et al*. Cyclophosphamide-Mediated Tumor Priming for Enhanced Delivery and Antitumor Activity of HER2-Targeted Liposomal Doxorubicin (MM-302). Mol Cancer Ther 2015;14(9):2060–2071. doi:10.1158/1535-7163.Mct-15-0314, PMID:26162690.